

Communication: Simple liquids' high-density viscosity

Lorenzo Costigliola,^{1,a)} Ulf R. Pedersen,¹ David M. Heyes,² Thomas B. Schröder,¹ and Jeppe C. Dyre^{1,b)}

¹*Glass and Time, IMFUFA, Department of Science and Environment, Roskilde University, P.O. Box 260, DK-4000 Roskilde, Denmark*

²*Department of Mechanical Engineering, Imperial College London, Exhibition Road, South Kensington, London SW7 2AZ, United Kingdom*

(Received 10 January 2018; accepted 12 February 2018; published online 27 February 2018)

This paper argues that the viscosity of simple fluids at densities above that of the triple point is a specific function of temperature relative to the freezing temperature at the density in question. The proposed viscosity expression, which is arrived at in part by reference to the isomorph theory of systems with hidden scale invariance, describes computer simulations of the Lennard-Jones system as well as argon and methane experimental data and simulation results for an effective-pair-potential model of liquid sodium. *Published by AIP Publishing.* <https://doi.org/10.1063/1.5022058>

The factors that affect the steady-state shear viscosity, η , of a fluid have been the subject of much investigation, yet no first-principles expression for the state-point dependence of η exists that allows for a straightforward calculation of η from the system's Hamiltonian. This means that one cannot easily calculate the viscosity's dependence on temperature T , particle number density $\rho \equiv N/V$, and pressure p for dense fluids. The literature is centered around semi-empirical expressions based on parameters such as the free volume that are not uniquely defined for real atoms and molecules, and viscosity data have typically been fitted to empirical polynomial expressions not obviously linked to the underlying physics.^{1–5} The density and temperature ranges where they are applicable are also limited.

A significant early development in providing an accurate expression for η is Enskog's expression for hard spheres,^{6,7}

$$\eta^* \equiv \frac{\eta}{\eta_0^{\text{HS}}} = \frac{1.016}{g(\sigma)} + 0.8B_2\rho + 0.7614g(\sigma)B_2^2\rho^2. \quad (1)$$

Here σ is the sphere radius and $B_2 = 2\pi\sigma^3/3$ is the second virial coefficient. The viscosity prefactor η_0^{HS} is given by

$$\eta_0^{\text{HS}}(T) = \frac{5}{16\sigma^2} \left(\frac{mk_B T}{\pi} \right)^{1/2}. \quad (2)$$

The mass of the sphere is m and k_B is the Boltzmann constant. The value of the radial distribution function at contact of the hard spheres is given by $g(\sigma) = (Z - 1)/(B_2\rho)$ in which $Z = p/\rho k_B T$ is the so-called compressibility factor.⁸ At liquid-like densities, the last term on the right-hand side of Eq. (1) dominates and is, apart from a numerical factor, the same as derived by Longuet-Higgins and Pople⁹ based on simple kinetic arguments.

The dimensionless viscosity η^* in Eq. (1) involves the effective molecule radius σ . This concept appears also in the

expression for the fluidity ($1/\eta$) of Dymond¹⁰ for high-density fluids in which the fluidity is taken to be linear in the volume per particle, v . A linear dependence on v was also considered by Hildebrand¹¹ and by van Loef,^{12,13} who showed that it fits well to the viscosity of dense fluids composed of a wide variety of molecules. The molecular diameter is typically expressed in terms of the close-packed volume per particle of the crystal. This prescription has been found to reproduce well also the fluidity of model inverse-power fluids.¹⁴

An alternative definition of the characteristic length scale is $\rho^{-1/3}$. This has been used in scaling onto a single curve the viscosity trends for high-density fluids¹⁵ and hydrocarbon fluids.^{16,17} Andrade in the 1930s proposed an early application of this type of viscosity scaling, for molten metals,^{18–20} which lead to the “macroscopically” reduced (dimensionless) viscosity,

$$\tilde{\eta} \equiv \rho^{-2/3}(mk_B T)^{-1/2}\eta. \quad (3)$$

Even though σ and $\rho^{-1/3}$ are numerically close for dense liquids, this substitution is a significant conceptual leap. It makes the transition from molecular-potential focused equations for transport coefficients, which trace their origin to the kinetic theory of gases and the hard-sphere model, to ones based on macroscopic variables independent of molecular detail and characteristics. This treatment is an important step towards including transport coefficients within the category of thermodynamic state functions.²¹

The idea that viscosity and thermodynamic properties are subject to the same treatment is implicit in a number of previous studies.^{21–23} Hoover *et al.*²⁴ showed theoretically that the density and temperature properties of model fluids formed by the inverse power-law pair potential, $v(r) \propto r^{-n}$, collapse onto a single curve where $\rho^{n/3}/T$ is constant. Alba-Simionesco, Roland, and their respective co-workers more recently showed that the experimental reduced dynamical properties of many glass-forming molecular liquids can be collapsed in the same way, treating the exponent n as a fitting parameter.^{25–27} The recent body of work on isomorph scaling has confirmed this

^{a)}lorenzo.costigliola@gmail.com

^{b)}dyre@ruc.dk

assumption and provided a theoretical basis.^{28–30} With isomorphs defined as the lines of constant excess entropy in the thermodynamic phase diagram,^{28,31} the reduced viscosity $\tilde{\eta}$ is constant along an isomorph because the reduced-unit dynamics is. This fact is not reliant on a particular form of the potential as long as the system has strong virial potential-energy correlations at the state points in question.²⁸ In particular, it is not restricted to inverse-power potentials or even to pair potentials, and several *molecular* systems have been shown to conform to the isomorph theory in computer simulations^{32,33} and experiments.^{34–36}

Not all systems have isomorphs, though. While most metals and van der Waals bonded liquids are believed to have isomorphs in the condensed-phase part of their phase diagram, systems with significant directional bonding like covalently or hydrogen-bonded systems are not expected to have isomorphs.^{32,37,38} The Lennard-Jones (LJ) liquid belongs to the former class of the so-called Roskilde (R)-simple systems,^{31,39–43} which includes most systems with more or less spherical interaction symmetry, the property that traditionally defines a “simple” system.⁸ We use below the isomorph theoretical framework as a guide to arrive at an expression for how simple liquids’ viscosity varies throughout the high-density part of the thermodynamic phase diagram. A novel viscosity expression is suggested with reference to the LJ system and shown to describe well experimental data for methane and argon as well as simulation data for an effective pair-potential model of liquid sodium.

R-simple systems are characterized by a potential-energy function $U(\mathbf{R})$ obeying the following scaling condition³¹ (in which \mathbf{R} is the $3N$ coordinates of the N particles and $\lambda > 0$ is a scaling factor):

$$U(\mathbf{R}_a) < U(\mathbf{R}_b) \Rightarrow U(\lambda\mathbf{R}_a) < U(\lambda\mathbf{R}_b). \quad (4)$$

Equation (4) is strictly obeyed only for an Euler-homogeneous potential plus a constant, but it is a good approximation for several realistic atomic and molecular models.^{31,44} For such systems, the scaling property is rarely obvious from the mathematical expression for $U(\mathbf{R})$ for which reason the term “hidden scale invariance” is sometimes used.^{28,33,45–49}

The R-simple region of a given system is identified in computer simulations as the state points characterized by strong virial potential-energy correlations in constant-volume canonical-ensemble fluctuations.^{28,50,51} For the LJ liquid, our simulations have shown that the Pearson correlation coefficient obeys $R > 0.94$ at all state points with density and temperature higher than those of the liquid at the triple point. Whenever Eq. (4) applies, the isomorphs are to a good approximation

invariance curves for both structure and dynamics^{28,31} if quantities have been made dimensionless using the “macroscopic” unit system with distance measured in units of $\rho^{-1/3}$, energy in units of $k_B T$, and time in units of $(m/k_B T)^{1/2} \rho^{-1/3}$.²⁸

In the simplest version of the isomorph theory,^{28,52} a function of density $h(\rho)$ exists for any R-simple system such that its isomorphs are given^{47,52} by

$$\frac{h(\rho)}{T} = \text{Const.} \quad (5)$$

For systems in three dimensions with pair potentials of the form $v(r) = \sum_n v_n r^{-n}$, the function $h(\rho)$ has one term for each inverse power-law term, $h(\rho) = \sum_n C_n \rho^{n/3}$.⁵² For the LJ pair potential $v_{\text{LJ}}(r) = 4\epsilon \left[(r/\sigma)^{-12} - (r/\sigma)^{-6} \right]$, one has if γ_0 is the so-called density-scaling exponent determined from a simulation at a single state point with density ρ_0 ⁴⁷

$$h_{\text{LJ}}(\rho) = \left(\frac{\gamma_0}{2} - 1 \right) \left(\frac{\rho}{\rho_0} \right)^4 - \left(\frac{\gamma_0}{2} - 2 \right) \left(\frac{\rho}{\rho_0} \right)^2. \quad (6)$$

Because $\tilde{\eta}$ is isomorph invariant, Eq. (5) implies that $\tilde{\eta}$ is a function of $h(\rho)/T$. If the temperature variation along a reference isomorph as a function of density is denoted by $T_0(\rho)$, Eq. (5) shows that $h(\rho) \propto T_0(\rho)$. Thus one can write $\tilde{\eta}(\rho, T) = F(T_0(\rho)/T)$.

The freezing line, which marks the limit between liquid and solid-liquid coexistence regions in the density-temperature phase diagram, defines a temperature function $T_F(\rho)$ in which ρ is the liquid density. The freezing line is an approximate liquid-state isomorph,^{28,53,54} implying that the reference isomorph function $T_0(\rho)$ may be taken to be $T_F(\rho)$,³⁰ i.e.,

$$\tilde{\eta}(\rho, T) = F(T_F(\rho)/T). \quad (7)$$

Rosenfeld applied this temperature scaling for the single-particle diffusion constant and the viscosity of the Yukawa system,⁵⁵ which is now known to be R-simple.⁴⁹ The function F in Eq. (7) is *a priori* system dependent, but the data presented below interestingly suggest that the same functional form applies for all simple liquids.

Simulations were carried out using Roskilde University Molecular Dynamics running on graphics processing units⁵⁸ (details are given in the [supplementary material](#)). At each state point in Fig. 1(a), a SLLOD simulation was run to evaluate the viscosity. Figure 1(b) shows viscosity data for the LJ liquid at the state points given in Fig. 1(a). Upon heating at constant density, the viscosity initially decreases and then increases. The existence of viscosity minima along isochores is well known.⁵⁹

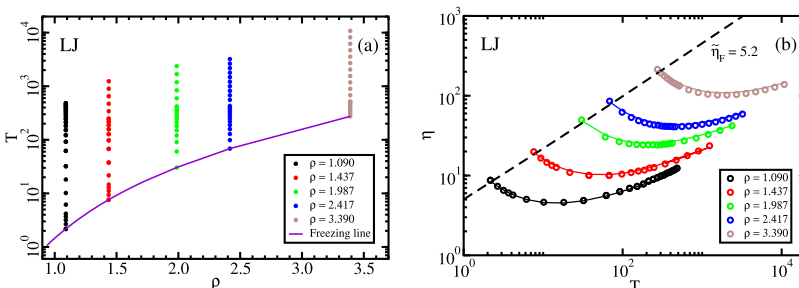


FIG. 1. Computer simulations of the Lennard-Jones (LJ) fluid at moderate and high densities relative to the triple point liquid density, which is 0.84 in the LJ units used here. (a) shows the state points simulated. The full curve is the freezing line.⁵⁶ (b) shows the viscosity calculated from SLLOD simulations⁵⁷ in which η is identified as the zero shear-rate limit of the shear-rate dependent viscosity (see the [supplementary material](#)). The full curves are the predictions of Eq. (10) (see below), and the dashed curve is the freezing line, which is characterized by the reduced viscosity $\tilde{\eta}_F = 5.2$.

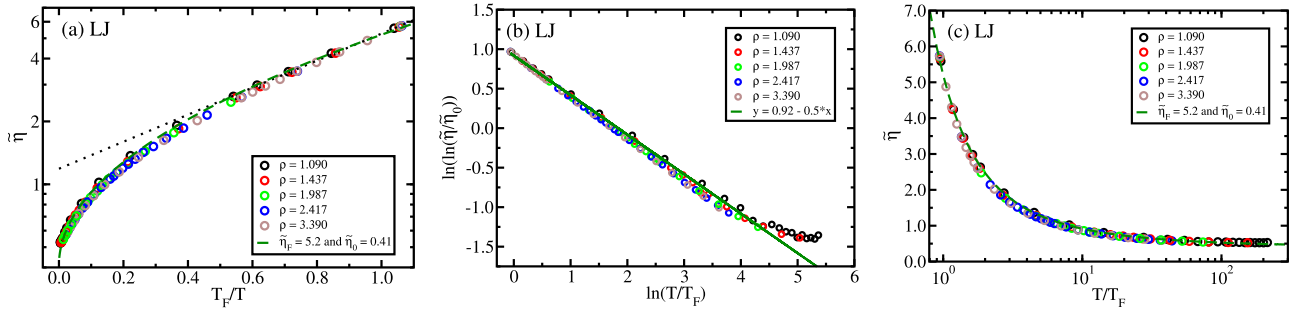


FIG. 2. The reduced viscosity $\tilde{\eta}$ of the LJ liquid. (a) shows the logarithm of $\tilde{\eta}$ as a function of freezing temperature over temperature for the data of Fig. 1(b). The approximately linear dependence observed close to the freezing line (dotted line) is consistent with Kaptay's expression, Eq. (9),⁶⁰ but there are systematic deviations from this at high temperatures. The barely visible green line represents Eq. (10), which is also given in (b) and (c). (b) tests Eq. (10) in a plot in which the line has slope $-1/2$ and $\tilde{\eta}_0$ is a free parameter. The data follow this line, except at the highest temperatures where the plot is very sensitive to the exact choice of $\tilde{\eta}_0$ (see the [supplementary material](#)). (c) Direct test of Eq. (10). The minor high-temperature deviations observed in (b) are not visible because the relevant reduced viscosities are close to the high-temperature plateau value $\tilde{\eta}_0$.

In order to validate Eq. (7) we proceed to identify an expression for the LJ system's freezing temperature as a function of density. A good overall representation of the freezing line is³⁰ (with density given in LJ units)

$$T_F(\rho) = 2.27\rho^4 - 0.80\rho^2. \quad (8)$$

An expression of this form was used by Rosenfeld in 1976⁶¹ and more recently by Khrapak and others.^{62,63} Since the freezing line is an approximate isomorph, for the LJ system the functional form Eq. (8) follows from Eq. (6).³⁰

Figure 2(a) plots the reduced viscosity of the LJ system as a function of $T_F(\rho)/T$ using Eq. (8) for $T_F(\rho)$. There is excellent collapse. Close to T_F we confirm the linear dependence of $\ln \tilde{\eta}$ on $T_F(\rho)/T$ predicted by Kaptay's

liquid-metal constant activation energy generalization of the Andrade equation⁶⁰ (dotted straight line),

$$\tilde{\eta} = \tilde{\eta}_0 \exp(CT_F(\rho)/T). \quad (9)$$

Systematic deviations from this are seen moving away from the freezing line, however.

Figure 2(b) investigates the functional form of F in Eq. (7) by plotting the logarithm of the reduced viscosity in a log-log plot with $\tilde{\eta}_0$ as a free parameter. Care must be exercised when subjecting data to two logarithms, but keeping this in mind the figure shows that for $\tilde{\eta}_0 = 0.41$ most data collapse onto a line with slope $-1/2$. This means that the LJ system's viscosity is well represented by the following expression:

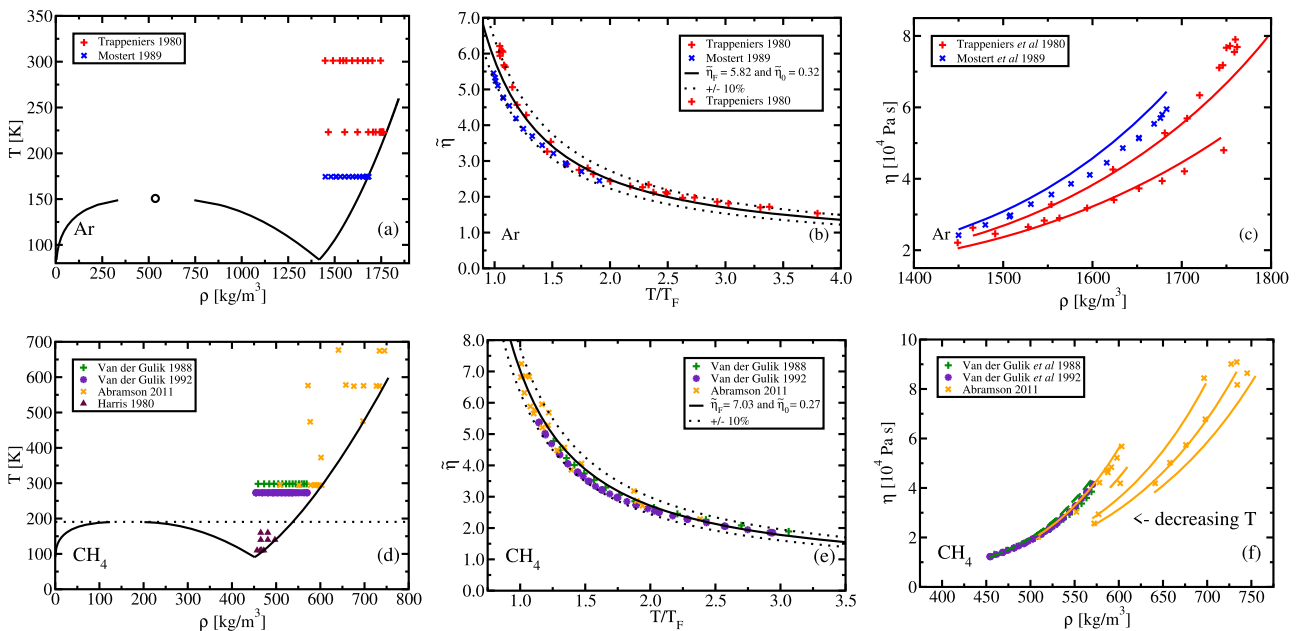
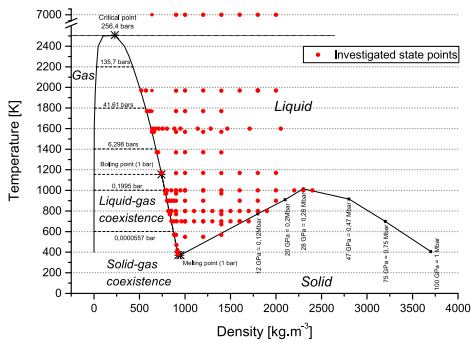
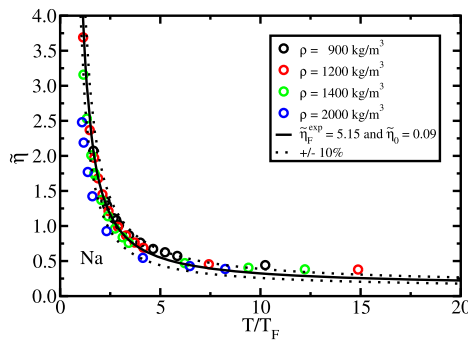


FIG. 3. Tests of the viscosity equation Eq. (10) against experimental data for argon^{64,65} and methane⁶⁶⁻⁶⁹ (upper and lower panels). (a) shows the state points at which argon's viscosity was measured. (b) shows argon's reduced viscosity as a function of $T/T_F(\rho)$ in which the full curve is Eq. (10). The viscosity is predicted correctly within 10% as indicated by the dotted lines. (c) shows argon's non-reduced viscosity as a function of density along different isotherms. The full curves are the predictions. (d) shows the state points at which methane's viscosity was measured. (e) shows methane's reduced viscosity as a function of $T/T_F(\rho)$ in which the full curve is the prediction of Eq. (10). The viscosity is predicted correctly within 10% as indicated by the dotted lines. (f) shows methane's non-reduced viscosity as a function of density along different isotherms. The full curves are the predictions.



(a)



(b)

$$\tilde{\eta}(\rho, T) = \tilde{\eta}_0 \exp \left[B \left(\frac{T_F(\rho)}{T} \right)^{1/2} \right]. \quad (10)$$

To validate this directly, Fig. 2(c) plots the reduced viscosity data as a function of $T/T_F(\rho)$ with Eq. (10) as the dashed green line. The full curves of Fig. 1(b) are the corresponding non-reduced viscosity predictions. Using instead of 1/2 the exponent 0.4⁵⁵ gives a worse fit; see the [supplementary material](#).

Equation (10) involves just two dimensionless parameters, $\tilde{\eta}_0$ and B . The reduced viscosity at freezing $\tilde{\eta}_F$ determines B via

$$B = \ln(\tilde{\eta}_F/\tilde{\eta}_0). \quad (11)$$

The two free parameters of Eq. (10) may be determined from one viscosity measurement at freezing and one measurement away from the freezing line. For the LJ system, we find $\tilde{\eta}_F = 5.2$ and $\tilde{\eta}_0 = 0.41$, corresponding to $B = 2.54$.

Figure 3 reproduces data for methane and argon in which Figs. 3(a) and 3(d) are density-temperature phase diagrams showing the state points at which the viscosity was measured. Figures 3(b) and 3(e) compare the reduced viscosity data with best fits to Eq. (10). In both cases, Eq. (10) reproduces the data within 10% (marked by the dashed lines). Finally, Figs. 3(c) and 3(f) compare the non-reduced viscosity data to the prediction along a few isotherms.

Recently, Meyer *et al.* simulated liquid sodium modeled by a density-dependent effective pair potential derived from the Fiolhais model of electron-ion interaction with self-consistent screening using a local field correction.⁷⁰ As is clear from Fig. 4, the reduced viscosity data of the sodium model conform well to Eq. (10).

Based on a hard-sphere argument, Andrade in 1934 derived an expression for the viscosity of liquids at freezing, which implied a constant reduced viscosity along the freezing line identified by the Lindemann melting criterion.⁷¹ In 2005, Kaptay generalized this expression to $\eta \propto m^{1/2} T^{1/2} V^{-2/3} \exp(CT_F/T)$, which is Eq. (9) in non-reduced units.⁶⁰ This expression was shown to work well for 18 metals at ambient pressure.⁶⁰ Equation (10) is qualitatively different by having $(T_F/T)^{1/2}$ instead of T_F/T in the exponential. The new viscosity equation represents data well in the region of the phase diagram studied by Kaptay and others, as well as at much higher temperatures.

In summary, Eq. (10) suggests a quasiuniversal viscosity expression for simple liquids,^{22,44,72} which reduces the

FIG. 4. Test of Eq. (10) for computer simulations of liquid sodium.⁷⁰ (a) shows the state points at which the viscosity was calculated. Reprinted with permission from N. Meyer, H. Xu, and J.-F. Wax, Phys. Rev. B **93**, 214203 (2016). Copyright 2016 American Physical Society. (b) shows the reduced viscosity data as a function of $T/T_F(\rho)$ in which the full curve is the prediction of Eq. (10). The dotted lines mark the viscosity $\pm 10\%$.

number of independent experiments/simulations needed to map out the viscosity as a function of state point in the phase diagram. Just two measurements of viscosity can now be used to predict its value throughout a fairly large liquid region of the phase diagram. This has potential applications in fields where the pressure can be very high, such as in some lubrication applications and magma geology. Obviously the chemical species there are more complicated than the small molecules considered in the present study. Nevertheless, the scaling treatment verified here may apply for more complex chemical systems and throw light on some important outstanding fundamental questions such as what is the viscosity of the Earth's outer core and how it varies with depth.^{73,74}

The argument leading to Eq. (10) was based in part on the isomorph theory which is, however, also consistent with Kaptay's expression Eq. (9). An important task for the future is to justify the temperature square root needed to fit data properly, which as far as we are aware is not yet derivable from theory. Another important task is to check Eq. (10) for more real liquids and computer-simulated simple liquids.

See the [supplementary material](#) for details on the computer simulations and comparisons of our findings to the viscosity expressions of van Loef, Longuet, and Rosenfeld, as well as showing that it is possible to use a reference isomorph that is not the melting line.

We thank Professor J.-F. Wax for making the numerical data of Ref. 70 available and are grateful to Vadim Brazhkin and Kenneth Harris for helpful correspondence. This work was supported by the VILLUM Foundation's Grant Nos. VKR-023455 and 16515 (Matter).

¹*Transport Properties of Fluids: Their Correlation, Prediction and Estimation*, edited by J. Millat, J. H. Dymond, and C. A. de Castro (IUPAC-Cambridge University Press, 1996).

²D. M. Heyes, *J. Chem. Soc., Faraday Trans. 2* **79**, 1741 (1983).

³D. M. Heyes, *Phys. Rev. B* **37**, 5677 (1988).

⁴J. V. Loef and E. Cohen, *Physica A* **156**, 522 (1989).

⁵H. O. Baled, I. K. Gamwo, R. M. Enick, and M. A. McHugh, *Fuel* **218**, 89 (2018).

⁶S. Chapman and T. G. Cowling, *The Mathematical Theory of Non-Uniform Gases: An Account of the Kinetic Theory of Viscosity, Thermal Conduction and Diffusion in Gases* (Cambridge University Press, 1970).

⁷H. Sigurgeirsson and D. M. Heyes, *Mol. Phys.* **101**, 469 (2003).

⁸J.-P. Hansen and I. R. McDonald, *Theory of Simple Liquids: With Applications to Soft Matter*, 4th ed. (Academic, New York, 2013).

- ⁹H. C. Longuet-Higgins and J. A. Pople, *J. Chem. Phys.* **25**, 884 (1956).
- ¹⁰J. H. Dymond, *J. Chem. Phys.* **60**, 969 (1974).
- ¹¹J. H. Hildebrand, *Science* **174**, 490 (1971).
- ¹²J. J. van Loef, *J. Phys. F: Met. Phys.* **4**, L190 (1974).
- ¹³J. J. van Loef, *Physica B+C* **103**, 133 (1981).
- ¹⁴D. M. Heyes, S. M. Clarke, and A. C. Branka, *J. Chem. Phys.* **131**, 204506 (2009).
- ¹⁵J. C. M. Li and P. Chang, *J. Chem. Phys.* **23**, 518 (1955).
- ¹⁶J. H. Dymond, *Physica* **75**, 100 (1974).
- ¹⁷J. H. Dymond, *Int. J. Thermophys.* **18**, 303 (1997).
- ¹⁸E. N. C. Andrade, *Nature* **128**, 835 (1931).
- ¹⁹E. N. C. Andrade, *London, Edinburgh, Dublin Philos. Mag. J. Sci.* **17**, 497 (1934).
- ²⁰E. N. C. Andrade, *London, Edinburgh, Dublin Philos. Mag. J. Sci.* **17**, 698 (1934).
- ²¹Y. Rosenfeld, *Phys. Rev. A* **15**, 2545 (1977).
- ²²Y. Rosenfeld, *J. Phys.: Condens. Matter* **11**, 5415 (1999).
- ²³H. A. Spikes, *Tribol. Trans.* **33**, 140 (1990).
- ²⁴W. G. Hoover, S. G. Gray, and K. W. Johnson, *J. Chem. Phys.* **55**, 1128 (1971).
- ²⁵C. Alba-Simionesco, A. Cailliaux, A. Alegria, and G. Tarjus, *Europhys. Lett.* **68**, 58 (2004).
- ²⁶C. M. Roland, S. Hensel-Bielowka, M. Paluch, and R. Casalini, *Rep. Prog. Phys.* **68**, 1405 (2005).
- ²⁷D. Coslovich and C. M. Roland, *J. Chem. Phys.* **130**, 014508 (2009).
- ²⁸N. Gnan, T. B. Schröder, U. R. Pedersen, N. P. Bailey, and J. C. Dyre, *J. Chem. Phys.* **131**, 234504 (2009).
- ²⁹J. C. Dyre, *J. Phys. Chem. B* **118**, 10007 (2014).
- ³⁰L. Costigliola, T. B. Schröder, and J. C. Dyre, *Phys. Chem. Chem. Phys.* **18**, 14678 (2016).
- ³¹T. B. Schröder and J. C. Dyre, *J. Chem. Phys.* **141**, 204502 (2014).
- ³²T. S. Ingebrigtsen, T. B. Schröder, and J. C. Dyre, *J. Phys. Chem. B* **116**, 1018 (2012).
- ³³A. A. Veldhorst, J. C. Dyre, and T. B. Schröder, *J. Chem. Phys.* **141**, 054904 (2014).
- ³⁴D. Gundermann, U. R. Pedersen, T. Hecksher, N. P. Bailey, B. Jakobsen, T. Christensen, N. B. Olsen, T. B. Schröder, D. Fragiadakis, R. Casalini, C. M. Roland, J. C. Dyre, and K. Niss, *Nat. Phys.* **7**, 816 (2011).
- ³⁵W. Xiao, J. Tofteskov, T. V. Christensen, J. C. Dyre, and K. Niss, *J. Non-Cryst. Solids* **407**, 190 (2015).
- ³⁶H. W. Hansen, A. Sanz, K. Adrjanowicz, B. Frick, and K. Niss, *Nat. Commun.* **9**, 518 (2018).
- ³⁷F. Hummel, G. Kresse, J. C. Dyre, and U. R. Pedersen, *Phys. Rev. B* **92**, 174116 (2015).
- ³⁸D. E. Albrechtsen, A. E. Olsen, U. R. Pedersen, T. B. Schröder, and J. C. Dyre, *Phys. Rev. B* **90**, 094106 (2014).
- ³⁹A. Malins, J. Eggers, and C. P. Royall, *J. Chem. Phys.* **139**, 234505 (2013).
- ⁴⁰E. Flenner, H. Staley, and G. Szamel, *Phys. Rev. Lett.* **112**, 097801 (2014).
- ⁴¹S. Prasad and C. Chakravarty, *J. Chem. Phys.* **140**, 164501 (2014).
- ⁴²M. Romanini, M. Barrio, R. Macovez, M. D. Ruiz-Martín, S. Capaccioli, and J. L. Tamarit, *Sci. Rep.* **7**, 1346 (2017).
- ⁴³G. Shrivastav, M. Agarwal, C. Chakravarty, and H. K. Kashyap, *J. Mol. Liq.* **231**, 106 (2017).
- ⁴⁴J. C. Dyre, *J. Phys.: Condens. Matter* **28**, 323001 (2016).
- ⁴⁵T. S. Ingebrigtsen, T. B. Schröder, and J. C. Dyre, *Phys. Rev. X* **2**, 011011 (2012).
- ⁴⁶T. B. Schröder, N. Gnan, U. R. Pedersen, N. P. Bailey, and J. C. Dyre, *J. Chem. Phys.* **134**, 164505 (2011).
- ⁴⁷L. Bøhling, T. S. Ingebrigtsen, A. Grzybowski, M. Paluch, J. C. Dyre, and T. B. Schröder, *New J. Phys.* **14**, 113035 (2012).
- ⁴⁸A. K. Bacher, T. B. Schröder, and J. C. Dyre, *Nat. Commun.* **5**, 5424 (2014).
- ⁴⁹A. A. Veldhorst, T. B. Schröder, and J. C. Dyre, *Phys. Plasmas* **22**, 073705 (2015).
- ⁵⁰N. P. Bailey, U. R. Pedersen, N. Gnan, T. B. Schröder, and J. C. Dyre, *J. Chem. Phys.* **129**, 184507 (2008).
- ⁵¹N. P. Bailey, U. R. Pedersen, N. Gnan, T. B. Schröder, and J. C. Dyre, *J. Chem. Phys.* **129**, 184508 (2008).
- ⁵²T. S. Ingebrigtsen, L. Bøhling, T. B. Schröder, and J. C. Dyre, *J. Chem. Phys.* **136**, 061102 (2012).
- ⁵³D. M. Heyes and A. C. Branka, *J. Chem. Phys.* **143**, 234504 (2015).
- ⁵⁴U. R. Pedersen, L. Costigliola, N. P. Bailey, T. B. Schröder, and J. C. Dyre, *Nat. Commun.* **7**, 12386 (2016).
- ⁵⁵Y. Rosenfeld, *J. Phys.: Condens. Matter* **13**, L39 (2001).
- ⁵⁶R. Agrawal and D. A. Kofke, *Mol. Phys.* **85**, 43 (1995).
- ⁵⁷D. J. Evans and G. P. Morriss, *Phys. Rev. A* **30**, 1528 (1984).
- ⁵⁸N. P. Bailey, T. S. Ingebrigtsen, J. S. Hansen, A. A. Veldhorst, L. Bøhling, C. A. Lemarchand, A. E. Olsen, A. K. Bacher, L. Costigliola, U. R. Pedersen, H. Larsen, J. C. Dyre, and T. B. Schröder, *SciPost Phys.* **3**, 038 (2017).
- ⁵⁹V. V. Brazhkin, Y. D. Fomin, A. G. Lyapin, V. N. Ryzhov, and K. Trachenko, *Phys. Rev. E* **85**, 031203 (2012).
- ⁶⁰G. Kaptay, *Z. Metallkd.* **96**, 24 (2005).
- ⁶¹Y. Rosenfeld, *Mol. Phys.* **32**, 963 (1976).
- ⁶²S. A. Khrapak and G. E. Morfill, *J. Chem. Phys.* **134**, 094108 (2011).
- ⁶³U. R. Pedersen, *J. Chem. Phys.* **139**, 104102 (2013).
- ⁶⁴N. Trappeniens, P. V. D. Gulik, and H. V. D. Hooff, *Chem. Phys. Lett.* **70**, 438 (1980).
- ⁶⁵R. Mostert, P. van der Gulik, and H. van den Berg, *Physica A* **156**, 921 (1989).
- ⁶⁶K. Harris and N. Trappeniens, *Physica A* **104**, 262 (1980).
- ⁶⁷P. van der Gulik, R. Mostert, and H. van den Berg, *Physica A* **151**, 153 (1988).
- ⁶⁸P. van der Gulik, R. Mostert, and H. van den Berg, *Fluid Phase Equilib.* **79**, 301 (1992).
- ⁶⁹E. H. Abramson, *Phys. Rev. E* **84**, 062201 (2011).
- ⁷⁰N. Meyer, H. Xu, and J.-F. Wax, *Phys. Rev. B* **93**, 214203 (2016).
- ⁷¹A. R. Ubbelohde, *Melting and Crystal Structure* (Clarendon, Oxford, 1965).
- ⁷²N. Meyer, H. Xu, and J.-F. Wax, *Phys. Rev. B* **96**, 094201 (2017).
- ⁷³F. D. Stacey, *Rep. Prog. Phys.* **68**, 341 (2005).
- ⁷⁴D. E. Smylie, V. V. Brazhkin, and A. Palmer, *Phys.-Usp.* **52**, 79 (2009).